

Global fit to the charged leptons DIS data: α_s , parton distributions, and high twists

S. I. Alekhin

Institute for High Energy Physics, Protvino, 142284, Russia

(October 2000)

Abstract

We perform the NLO QCD analysis of the world data on inclusive deep inelastic scattering cross sections of charged leptons off the proton and the deuterium targets. The parton distributions, the value of strong coupling constant α_s , and the twist 4 contributions to the structure functions F_2 and F_L are extracted with the complete account for the correlations of data points due to the systematic errors. Sensitivity of the α_s value and the high twist contribution to the procedures of accounting for the systematic errors is studied. The impact of theoretical uncertainties on the value of α_s and on the parton distributions is analysed. The obtained value of strong coupling constant with the account of these uncertainties is $\alpha_s(M_Z) = 0.1165 \pm 0.0017(\text{stat} + \text{syst}) \pm_{0.0034}^{0.0026}(\text{theor})$. The uncertainties of parton-parton luminosities for the FNAL and LHC colliders are estimated.

PACS number(s): 13.60Hb,12.38Bx,06.20.Jr

I. INTRODUCTION

Experiments on deep inelastic scattering (DIS) of leptons off nucleons is a unique source of information about strong interaction. These experiments were initiated at SLAC linac and later were continued at different accelerators using the fixed targets and the colliding electron-proton beams. The data for proton and deuterium targets, given in Refs. [1–4] are especially valuable, since no heavy-nucleus corrections are needed for their interpretation. Those data combined with the results from HERA electron-proton collider [5,6] allows one to determine the parton distribution functions (PDFs) and are widely used for this purpose. In particular, global fits of PDFs, which are regularly updated by collaborations MRST [7] and CTEQ [8], rely heavily on the DIS data. It is often mentioned, that the MRST and CTEQ PDFs lack information on uncertainties, that does not allow one to estimate the uncertainties on the cross sections, which are calculated using those PDFs. Most often these uncertainties are estimated as a spread of results, obtained using different PDFs sets. Meanwhile, it is evident, that if different PDFs are based on the same theoretical model fitted to a similar data sets, this spread mainly reflects uncertainties of calculations, rather, than real uncertainties arising from statistical and systematic errors on the data used for the extraction of PDFs. Besides, those collaborations combine statistical and systematic errors in quadrature, i.e. do not account for the correlation of the latter. Since systematic errors dominate over statistical ones for many DIS experiments, they govern total experimental errors on the PDFs parameters fitted to the data and ignorance of their correlations may lead to the distortion of the parameters errors and to the bias of their central values.

Statistical and systematic errors are combined in quadrature in part by historical reasons. The other reason is that, contrary to the case of statistical errors, existing approaches to the account of systematic errors are not so straightforward and encounter with technical difficulties generated by correlations between measurements, which become more significant when the systematic errors rise, as compared with the statistical ones. Nevertheless, as it was shown in Ref. [9] on the example of combined analysis of DIS data from Refs. [2,3,5,6] with the complete account of correlations due to systematic errors, these difficulties can be overcome using in the fit an estimator based on the covariance matrix. The results of the combined analysis of data from Refs. [1–6], which attempted to account for correlations of systematic errors, was later given in Ref. [10], but due to the large number of independent sources of the systematic errors, they were combined with the statistical errors partially. Regardless of the expressed confidence that this procedure should have minimal impact on the results, this point is not ultimately clarified and it is evident that errors on the obtained PDFs may be distorted.

In this paper we describe the results of the combined analysis of the world data on the charged leptons DIS off the proton and deuterium targets given in Refs. [1–6]. In comparison with our previous fit of Ref. [9] in the present analysis we use data with lower values of transferred momentum Q . Besides, the data from the SLAC experiments and the experiment FNAL-E-665 are added. As well as in Ref. [9], we extract from the data the nucleon PDFs and the value of strong coupling constant α_s . In addition, wealth of data at low Q allows one to determine the high twist (HT) contributions to the structure functions F_2 and F_L as well. Analysis is performed in the NLO QCD approximation with the complete account of correlations due to systematic errors within approach described in Ref. [11].

II. THE DIS PHENOMENOLOGY

It is well known that the DIS cross section of charged leptons off nucleons can be expressed in terms of structure functions $F_{2,3,L}$ ¹. For example, at 4-momentum transfers Q less, than the Z -boson mass the charged leptons cross section reads

$$\frac{d^2\sigma}{dx dy} = \frac{4\pi\alpha^2(s - M^2)}{Q^4} \left[\left(1 - y - \frac{(Mxy)^2}{Q^2} \right) F_2 + \left(1 - 2\frac{m_l^2}{Q^2} \right) \frac{y^2}{2} (F_2 - F_L) \right], \quad (2.1)$$

where s is the s.c.m. energy, m_l is the lepton mass, y is the ratio of the energy lost by lepton to the initial lepton energy, x is the Bjorken scaling variable, M is the nucleon mass, α is the electro-magnetic coupling constant. The structure functions $F_{2,L}$ depend on the variables x and Q . Within the operator product expansion [13] the structure functions are given by the sum of contributions coming from operators of different twists. For the unpolarized lepton scattering the even twists larger or equal to two contribute only. Thus with the account of the twist-4 contribution

$$F_{2,L}(x, Q) = F_{2,L}^{\text{LT,TMC}}(x, Q) + H_{2,L}(x) \frac{1 \text{ GeV}^2}{Q^2}, \quad (2.2)$$

where $F_{2,L}^{\text{LT,TMC}}$ gives the leading twist (LT) with the account of target mass corrections, as calculated in Ref. [14]:

$$F_2^{\text{LT,TMC}}(x, Q) = \frac{x^2}{\tau^{3/2}} \frac{F_2^{\text{LT}}(\xi_{\text{TMC}}, Q)}{\xi_{\text{TMC}}^2} + 6 \frac{M^2 x^3}{Q^2 \tau^2} I_2, \quad (2.3)$$

$$F_L^{\text{LT,TMC}}(x, Q) = F_L^{\text{LT}}(x, Q) + \frac{x^2}{\tau^{3/2}} (1 - \tau) \frac{F_2^{\text{LT}}(\xi_{\text{TMC}}, Q)}{\xi_{\text{TMC}}^2} + \frac{M^2 x^3}{Q^2 \tau^2} (6 - 2\tau) I_2, \quad (2.4)$$

where

$$I_2 = \int_{\xi_{\text{TMC}}}^1 dz \frac{F_2^{\text{LT}}(z, Q)}{z^2},$$

$$\xi_{\text{TMC}} = \frac{2x}{1 + \sqrt{\tau}}, \quad \tau = 1 + \frac{4M^2 x^2}{Q^2},$$

and $F_{2,L}^{\text{LT}}$ are the structure functions of twist 2. Such approach allows us to separate pure kinematical corrections, so that the functions $H_{2,L}(x)$ correspond to “genuine” or “dynamical” contribution of the twist 4 operators. Note, that the parametrization (2.2) implies, that the anomalous dimensions of the twist 4 operators are equal to zero, that is invalid in general case. Moreover, there are attempts to estimate these anomalous dimensions from the

¹The comprehensive analysis of lepton-nucleon scattering amplitudes, including notations used throughout our paper is given, e.g., in review [12].

account of the correlations between partons (see Ref. [15]). Meanwhile, in view of limited precision of the data, approximation (2.2) is rather good (see also discussion in Ref. [16]).

The leading twist structure functions can be expressed in factorized form as the Mellin convolution of PDFs q with the coefficient functions C :

$$F_{2,L}^{\text{LT}}(x, Q) = \sum_i \int_x^1 \frac{dz}{z} C_{2,L}^i [z, \alpha_s(\mu_R), Q/\mu_F] q_i(x/z, \mu_F), \quad (2.5)$$

where index i marks the partons species and α_s is running strong coupling constant. The dependence of PDFs on Q is described by the DGLAP evolution equations [17]

$$Q \frac{\partial q_i(x, Q)}{\partial Q} = \sum_j \int_x^1 \frac{dz}{z} P_{ij} [z, \alpha_s(\mu_R), Q/\mu_R] q_j(x/z, Q), \quad (2.6)$$

and the PDFs evolution is governed by the splitting functions P_{ij} , which in turn depend on α_s . The quantities μ_F and μ_R in Eqs.(2.5) and (2.6) give the factorization and renormalization scales respectively. In the $\overline{\text{MS}}$ renormalization-factorization scheme, used in our analysis, these scales are chosen equal to the value of Q usually. The splitting and coefficient functions can be calculated in perturbative QCD as series in α_s . For the coefficient functions these series are completely calculated up to the next-to-next-to-leading order (NNLO) [18]; for the splitting functions the next-to-leading order (NLO) corrections are known, while for the NNLO corrections a limited set of the Mellin moments [19], as well as some asymptotes, are available only (see references in [20]). Nevertheless, there are attempts to analyse the DIS data in the NNLO QCD approximation with the consideration of the available moments only [21–23], or modelling splitting functions [24]. Our analysis is performed in the NLO QCD approximation with the use of the splitting and coefficient functions in x -space as they are given in Ref. [25].

The dependence of α_s on Q is given by the renormalization group equation, which in the NLO QCD approximation reads²:

$$\frac{1}{\alpha_s(Q)} - \frac{1}{\alpha_s(M_Z)} = \frac{\beta_0}{2\pi} \ln \left(\frac{Q}{M_Z} \right) + \beta \ln \left[\frac{\beta + 1/\alpha_s(Q)}{\beta + 1/\alpha_s(M_Z)} \right], \quad (2.7)$$

where $\beta = \frac{\beta_1}{4\pi\beta_0}$, β_0 and β_1 are regular coefficients of β -function: $\beta_0 = 11 - (2/3)n_f$, $\beta_1 = 102 - (38/3)n_f$, n_f is the number of active fermions, which depends on Q . In our analysis n_f was chosen equal to 3 for $Q \leq m_c$, 4 for $m_c \leq Q \leq m_b$, and 5 for $m_b \leq Q \leq m_t$, where m_c, m_b, m_t are masses of the c -, b - and t -quarks correspondingly, and when n_f changes, the continuity of $\alpha_s(Q)$ is kept (see Ref. [27] for argumentation of this approach). The choice of the quark mass value as the threshold for n_f switching is optional. E.g., in the analysis of heavy quark contribution to the DIS sum rules, given in Ref. [28], this threshold is chosen equal to $6.5m_{c,b,t}$. Unfortunately any choice cannot be completely justified, while

²Analogous equations given in Refs. [9,26] contain misprints, meanwhile, the calculations were performed using the correct Eqn.(2.7).

the dependence of results on the variation of threshold, say in the interval from $m_{c,b,t}$ to $6.5m_{c,b,t}$, generates one of the sources of theoretical uncertainties inherent to this analysis. Since the value of α_s depends on the threshold position logarithmically, for estimation of this uncertainty we shifted this threshold value to the logarithmic centre of this interval, i.e. from $m_{c,b,t}$ to $\sqrt{6.5}m_{c,b,t}$. Very often, approximate solutions of Eq.(2.7), based on the expansions of α_s in inverse powers of $\ln(Q)$ are used in calculation. Inaccuracy of these expansions for evolution of α_s from $O(\text{GeV})$ to M_Z may be as large as 0.001 [29], which is comparable with the experimental uncertainties of the $\alpha_s(M_Z)$ value extracted from the data. In order to escape these uncertainties we use in the analysis the exact numerical solution of Eq.(2.7) instead.

Since we use the truncated perturbative series, the results depend on the factorization scale μ_F and the renormalization scale μ_R . These dependences cause additional theoretical uncertainties of the analysis. The accurate estimate of these uncertainties is difficult, because the possible range of the scales variation is undefined and besides, one is to change factorization scheme as well. In our analysis we estimate only the theoretical uncertainty due to the choice of μ_R in the evolution equations (2.6) using the approach described in Ref. [30]. In accordance with this approach the renormalization scale μ_R is chosen equal to $k_R Q$ and the NLO evolution equations are modified in the following way

$$Q \frac{\partial q_i(x, Q)}{\partial Q} = \frac{\alpha_s(k_R Q)}{\pi} \sum_j \int_x^1 \frac{dz}{z} \left\{ P_{ij}^{(0)}(z) + \frac{\alpha_s(k_R Q)}{2\pi} [P_{ij}^{(1)}(z) + \beta_0 P_{ij}^{(0)}(z) \ln(k_R)] \right\} q_j(x/z, Q),$$

where $P^{(0)}$ and $P^{(1)}$ are respectively the LO and NLO coefficients of the splitting functions series. The change of results under variation of k_R from 1/2 to 2 gives an estimate of the error due to renormalization scale uncertainty. Evidently that, by definition, this uncertainty is connected with the impact of unaccounted terms of the perturbative series.

In order to obtain the PDFs from evolution equations, one is to supply a boundary conditions at some starting value Q_0 . The x -dependence of PDFs cannot be calculated from the modern strong interaction theory, it is determined from the comparison with data. Usual parametrization of the PDFs at Q_0 reads

$$xq_i(x, Q_0) = x^{a_i}(1-x)^{b_i}.$$

For this parametrization the behaviour of q at low x is motivated by the Regge phenomenology (see, e.g., book [31]) and at high x , by the quark counting rules [32,33]. If such a simple form is insufficient for the fair data description, polynomial-like factors are added. Value of Q_0 is arbitrary, but it is natural to choose it as $O(\text{GeV})$ to allow for simple interpretation of the boundary PDFs. Meanwhile, it was recently shown in Ref. [34], that the choice of Q_0 is important to provide the results stable with respect to the account of higher order QCD corrections (see also Ref. [22]). At low Q_0 the twist 4 contribution extracted from the data is less sensitive to the choice of the renormalization scale μ_R in Eq. (2.6), than at high Q_0 . The $\alpha_s(M_Z)$ behaves in opposite way, and then the choice $Q_0^2 = 9 \text{ GeV}^2$, made in our analysis, provides stability of the α_s and PDFs values if the NNLO QCD corrections are considered.

Despite of the fact, that the evolution equations have been used in the DIS data analysis for many years, no unique approach for solving them exists. Analytical expressions can be

obtained only for the simplified splitting functions, and direct numerical approaches demand threefold integration, which is time consuming. There are semi-analytical approaches, based on expansion of PDFs in terms of selected sets of functions, but such approaches, as a rule, lead to loosing of the universality with respect to the choice of splitting functions and require careful control of the calculations precision. Due to the form of the evolution equation kernel is rather complicated, correct implementation of a sophisticated integration algorithm meets the difficulties. In the comparative analysis of different codes, used for the DGLAP equations integration, the codes of the CTEQ and MRST collaborations were found to contain the bugs (see Ref. [35]). Taking into account these points, we use in the analysis our own code for direct numerical integration of Eq.(2.6), based on the Euler predictor-corrector algorithm (see Ref. [36]). This code allows one to modify kernels of the evolution equations in order to debug the code, to control the calculation precision, to take into account effects of new physics, and to implement special cases of evolution. Integration region can be expanded easily, and the integration precision is regulated by the external parameters of the code. For typical values of these parameters the code integration precision, as estimated using benchmark described in Ref. [35], is given in Fig. 1. One can see that the relative precision is better, than 0.001 in the region $x \lesssim 0.5$ and better, than 0.01 in the region $x \gtrsim 0.5$. This is well enough for our purposes, since the errors on data are larger, than the integration errors for all x .

Since Eq.(2.6) is valid for massless partons only, the heavy quarks contribution, which is significant at low x , should be considered in a peculiar way. In the approach described in Ref. [37] the heavy quarks are considered as massless ones. They are included into the general evolution starting from a threshold value of Q , which is proportional to the quark mass, while at the values of Q lower the threshold these distributions are put to zero. Evidently, in this approach the heavy quarks contribution is overestimated in the vicinity of the threshold. Alternative way to consider the heavy quarks contribution is to calculate it using the photon-gluon fusion model of Ref. [38]. At high Q and low x “large logarithms” arise in the elementary cross section of this process, that may demand its resummation [39]. Meanwhile, as it was shown in Ref. [40], the region of x and Q , where the resummation is really needed lays outside the region of the available DIS data. For this reason we calculated the c - and b - quarks contributions to the structure functions $F_{2,L}$ using the photon-gluon fusion model with the NLO coefficient functions of Ref. [41] and the renormalization/factorization scales equal to $\sqrt{Q^2 + 4m_{c,b}^2}$ at the quark masses $m_c = 1.5$ GeV and $m_b = 4.5$ GeV.

The LT contribution to the DIS structure functions is rather well understood both from theoretical and experimental points of view. Since this contribution depends on Q weakly one can reject the low Q data points and leave the data set, which is both statistically significant, and can be analysed within perturbative QCD in order to determine the LT x -dependence. The HT contribution is worse known, than the LT one. The theoretical analysis of the HT x -dependence is equally difficult as for the LT x -dependence and, as a result, it should be determined from data. Meanwhile, due to the fast fall of the HT contribution with Q it is significant for $Q^2 \lesssim 10$ GeV² only. At very low Q the subtraction of the LT contribution, as calculated in perturbative QCD is problematic due to the rise of α_s . As a result, only the data for $Q^2 \lesssim 1$ GeV² Q can be used for the HT extraction and the results precision is poor.

Study of the possibility to separate the HT and LT contributions has a long history (see Refs. [42–45]). Despite of that the Q -dependences of these contributions are different, in the limited range of Q the HT power corrections can simulate the logarithmic LT behaviour [46]. Moreover, as it was shown in Refs. [43,47], the power corrections can almost entirely describe the scaling violation observed for the DIS data, if the data precision is limited. In particular, this causes large correlations between the fitted values of α_s and the HT contribution. This correlation leads to the rise of the fitted parameters errors. The rise of errors is unpleasant effect, moreover, the fitted model non-linearity can become essential as a result. Besides, the fit results become less stable with respect to the change of the non-fitted parameters and adoptions of the fitted model, i.e., the theoretical errors on the fitted parameters rise also. Finally, if large correlations between parameters occur, the second derivative matrix for the minimized functional is poor determined and the calculations inaccuracies increase when its inversion. For this reason in order to get satisfactory precision of the parameters errors one is to guarantee better precision of the fitted model calculation, which may be time consuming, if manifold integration is involved. Due to this is the case for our analysis, estimation of the correlation coefficients between the fitted values of α_s and the HT contribution is non-trivial problem.

III. DATA USED IN THE FIT AND STARTING PDFS

We fit the PDFs to the data on the charged leptons DIS off proton and deuterium given in Refs. [1–6]. The data points with $Q^2 < 2.5 \text{ GeV}^2$ were not used in the analysis in order to reject the region, where α_s is rather large and the NNLO order QCD correction may be important. The points with $x > 0.75$, for which the nuclear corrections are large, were removed also. The data used in the analysis occupy the region $10^{-4} \lesssim x \leq 0.75$, $2.5 \text{ GeV}^2 \leq Q^2 \lesssim 5000 \text{ GeV}^2$. The number of data points for each experiment is given in Table I.

The starting PDFs were initially parametrized at $Q_0^2 = 9 \text{ GeV}^2$ as follows:

$$xq_i(x, Q_0) = A_i x^{a_i} (1-x)^{b_i} (1 + \gamma_1^i \sqrt{x} + \gamma_2^i x) \quad (3.1)$$

and then the parameters γ , which agree with zero within errors, were by turn fixed at zero till such parameters existed. Evidently, the fit quality could not get worse, when such parameters are fixed. The PDFs functional form resulted from this simplification and used in the final fit reads:

$$xu_V(x, Q_0) = \frac{2}{N_u^V} x^{a_u} (1-x)^{b_u} (1 + \gamma_2^u x),$$

$$xu_S(x, Q_0) = \frac{A_S}{N_S} \eta_u x^{a_{su}} (1-x)^{b_{su}},$$

$$xd_V(x, Q_0) = \frac{1}{N_d^V} x^{a_d} (1-x)^{b_d},$$

$$xd_S(x, Q_0) = \frac{A_S}{N^S} x^{a_{sd}} (1-x)^{b_{sd}},$$

$$xs_S(x, Q_0) = \frac{A_S}{N^S} \eta_s x^{a_{ss}} (1-x)^{b_{ss}},$$

$$xG(x, Q_0) = A_G x^{a_G} (1-x)^{b_G} (1 + \gamma_1^G \sqrt{x} + \gamma_2^G x),$$

where u, d, s, G are the up, down, strange quarks, and gluons distributions respectively; indices V and S correspond to the valence and sea quarks. The parameters N_u^V, N_d^V and A_G were not fitted, instead they were calculated from the other parameters using the conservation of the partons momentum and the fermion number. The parameter N^S was calculated using the relation

$$2 \int_0^1 x [u_s(x, Q_0) + d_s(x, Q_0) + s_s(x, Q_0)] dx = A_S.$$

It is well known, that the charged leptons data do not allow to confine the sea quarks contribution. For this reason the parameter η_s was fixed at 0.42, which agrees with the recent results of the NuTeV collaboration, given in Ref. [48]. The other sea distributions parameters were constrained as $a_{su} = a_{sd} = a_{ss}$, $b_{ss} = (b_{su} + b_{sd})/2$.

The DIS cross sections calculated from the QCD evolved PDFs using Eq.(2.1) with the account of the TMC corrections given by Eq.(2.3) and the twist 4 contribution in additive form as in Eq.(2.2), were fitted to the cross section data³. The HT contributions to the proton and neutron structure functions F_2 were parametrized by separate functions H_2^p and H_2^n respectively, and the HT contributions to the proton and neutron structure functions F_L , by the common function H_L^N , since the latter coincide within errors. The functions $H_2^{p,n}$ and H_L^N were parametrized in the model independent way: at $x = 0., 0.1, \dots 0.8$ their values were fitted to the data, and between these point the functions were linearly interpolated. The common approach for the PDFs global fits is to use data on F_2 instead of the data on cross sections. Within this approach one ignores the fact, that the F_2 values given by different experiments are often extracted from the cross sections using different values of F_L . In our fit the F_L contribution to the cross section was calculated iteratively and, efficiently, the data were reduced to the common value of F_L . Since the F_L contribution rises with y , the effect of this reduction is more important at high y . Due to the collision energy of each experiment is limited, the highest values of y correspond to the minimal values of x . For this reason the F_2 data points shifts due to the reduction to the common value of F_L are not very significant in average, but at the edges of the experiments data regions may reach several percents. Note, that at low x the F_L value strongly depends on the gluon distribution and, hence, in the fit to the cross sections data an additional constraint for the gluon distribution occurs, i.e. it is better confined, as compared to the fit to the F_2 data.

³Since the high Q data from the H1 and ZEUS experiments were corrected for the Z -boson contribution, Eq.(2.1) is applicable for these data also.

The TMC correction is most important for the SLAC data, less important for the BCDMS data, almost unimportant for the NMC data, and negligible for the others. Note, that our TMC correction to F_2 given by Eq.(2.3) differs from that applied in Ref. [49], where the substitution

$$F_2^{\text{LT,TMC}}(x, Q) = F_2^{\text{LT}}(\xi_{\text{TMC}}, Q) \quad (3.2)$$

was used to account for the target mass effect. The numerical difference between these two approaches is maximal at high x and low Q , e.g., for the SLAC data it reaches 40%. Besides, our TMC correction, contrary to that given by Eq.(3.2), changes sign at $x \approx 0.5$.

The deuterium data were corrected for the Fermi motion effect as in the model of Ref. [50] with the deuterium wave function from Ref. [51]. The deuterium correction value rises with x and reaches 16% for the SLAC data. This correction was calculated iteratively in the fit to provide consistency of the analysis. The two-dimensional integrals involved in the model were calculated using the code of Ref. [52], which provides better numerical stability, than the standard codes based on the Gauss integration algorithm. For the calculations time saving we adopted, that the Fermi motion correction for the structure function $xF_1 = F_2 - F_L$ is the same, as for the structure function F_2 (we checked that this adoption does not significantly affect the results).

IV. FITTING PROCEDURE AND RESULTS

The fitted parameters including the PDFs parameters, the value of α_s , and the coefficients of the functions $H_{2,L}$ were determined from the minimization of the functional

$$\chi^2 = \sum_{K,i,j} (f_i - \xi_K y_i) E_{ij} (f_j - \xi_K y_j), \quad (4.1)$$

where E_{ij} is inverse of the covariance matrix C_{ij} ,

$$C_{ij} = \xi_K^2 \delta_{ij} \sigma_i \sigma_j + f_i f_j (\vec{\eta}_i^K \cdot \vec{\eta}_j^K),$$

index K runs through the data subsets corresponding to the different experiments and the different targets within one experiment, indices i, j run through the data points in these subsets. The other notations: y_i are the measurements; σ_i are the statistical errors; ξ_K are the renormalization factors; f_i are the fitted model calculations depending on the fitted parameters; $\vec{\eta}_i^K$ are the systematic errors vectors (the dimensions of these vectors for each experiment are given in Table I as NSE). The systematic errors were considered as multiplicative, that is natural way for the counting experiments. All systematic errors, excluding the normalization errors on the old SLAC experiments, were accounted for in the covariance matrix. The data from the old SLAC experiments, as they were given in Ref. [1], are the result of re-analysis of the original experimental data published earlier (for the details see Ref. [53]). One of the purposes of this re-analysis was to renormalize the old data on the data from dedicated experiment SLAC-E-140. However, due to the latter did not release the proton target data, the renormalization of the proton data was performed using the experiment SLAC-E-49B as a “bridge”. Such technique certainly brings additional

uncertainties on the re-analysed data. In order to escape those uncertainties we performed the independent renormalization of the old SLAC experiments without a “bridging”, that is possible in our case, since we use more proton data, than in the analysis of Ref. [1]. For this purpose we fitted the factors ξ_K for each target of each old SLAC experiment independently. Alongside, to keep the analysis consistency the errors due to normalization uncertainties of the old SLAC experiments, given in Ref. [1], were cancelled out. For other experiments the parameters ξ_K were fixed at 1. The asymmetrical systematic errors on the ZEUS data were symmetrized, when including in the covariance matrix, and systematic errors on the BCDMS data for the proton and deuterium targets were considered as perfectly correlated.

The statistical properties of the estimator based on covariance matrix (CME) were considered in Ref. [11] in comparison with the statistical properties of the simplest χ^2 estimator (SCE), based on the minimization of the functional

$$\chi^2 = \sum_i \frac{(f_i - y_i)^2}{\sigma_i^2},$$

which is often used in particle physics for the analysis of data including the correlated ones as well. For the CME the fitted parameters systematic errors due to the data systematic errors are automatically included in the total error; for SCE the parameters systematic errors are estimated as the shift of the parameters under the shift of the data by the value of their systematic errors. The SCE dispersion is always larger, than the CME dispersion and, as it was shown in Ref. [11], the ratio of these dispersions can reach several units for realistic cases. It was shown also, that the CME is unbiased if the systematic errors on the parameters are not much more, than the statistical ones. In order to control the estimator bias one can trace the value of the net residual R , equal to the mean of weighted residual $(f - y)/\sqrt{\sigma^2 + (f\eta)^2}$. The χ^2 values and the net residuals for the total data set and for each experiment separately calculated at the parameters values fitted using the CME are given in Table I. One can see, that the net residual value is within its standard deviation⁴ and the data description is good, excluding description of the ZEUS data. For more detailed analysis of the confidence of the ZEUS data description we calculated for those data the diagonalized residuals r^D using the relation

$$r_i^D = \sum_{j=1}^N \sqrt{E_{ij}}(f_j - y_j),$$

where indices i, j run through the data points. If data are well described by fitted model, then for large N the values of r_i^D obey the normal distribution, i.e. the Gauss distribution with zero mean and the dispersion equal to 1. The distribution of r_i^D for the ZEUS data is given in Fig. 2. Evidently it does not agree with the normal distribution, that is not surprising, since the data description is poor. Note, that the diagonalized residuals mean is small for the ZEUS data (0.05), meanwhile, the dispersion is equal to 2.1, i.e. it is far from the normal distribution dispersion. It is difficult to ascribe this discrepancy to the shortcoming of the

⁴The R standard deviation was calculated using Eq. (3.11) from Ref. [11].

fitted model, since, as it seen from Fig. 2, analogues distribution for the H1 data agrees with the normal distribution perfectly, whereas both experiments gained similar statistical and kinematical coverage. One more possible explanation of this disagreement is, that the systematic errors given by the ZEUS collaboration are underestimated, but still are Gaussian distributed. In such cases the PDG scales the errors so that χ^2/NDP becomes equal to 1 (see review [29]). In our case this approach cannot be used, since number of independent sources of the systematic errors in the ZEUS experiment is large and a lot of variants of such rescaling can be applied. Besides, the distribution of residuals would remain non-Gaussian after the errors rescaling (see dashed curve in Fig. 2). Driven by this consideration one can suppose that systematic errors on the ZEUS data are non-Gaussian distributed (but with zero mean) and then χ^2/NDP must not be equal to 1. If so, the fitted parameters, which are confined by the ZEUS data, also may be distributed in arbitrary way (see in this connection Ref. [54]). Due to exact estimation of the confidence intervals for unknown distribution is impossible, we recommend for this purpose, in particular for evaluating the PDFs errors at low x , the robust estimate of the confidence intervals, based on the Chebyshev inequality (see discussion in Ref. [11]).

The dispersion of the net residual R is maximal for the SLAC-E-140, BCDMS, and NMC data sets. (Remind, that this dispersion rises with the increase of data correlation, full correlation corresponds to the dispersion of R equal to 1). Thus, one can conclude, that the account of the BCDMS and NMC data correlations has the largest impact on the analysis results, since number of points in the SLAC-E-140 data set is small. This conclusion is in line with the results of Ref. [26], where it was obtained, that in the combined fit to the non-singlet SLAC-BCDMS data the account of the BCDMS data correlations leads to much more significant shift of the parameters, than the account of the SLAC data correlations. The value of R for the total data set is well within its standard deviation, that confirms the fit unbiasedness.

The fitted PDFs parameters are given in Table II. We underline, that in our fit the universality of the valence u - and d -quarks behaviour at low x is not initially assumed, contrary to the popular global fits practice, and the fit results confirm this universality with the few percents precision. At the same time the Regge phenomenology prediction (see, e.g., book [31])

$$a_u = a_d = 0.5 \tag{4.2}$$

is in disagreement with the fit results⁵. A possible interpretation of this disagreement is, that Eq.(4.2), as it is deduced, is not related to a particular value of Q , while the QCD evolution does change the PDFs x -behaviour. As it was shown in Ref. [55], for the non-singlet distributions at low x this change is not very significant, but at least partially it can help to explain the observed disagreements. The values of the parameters a_u and a_d agrees with the results of our earlier analysis of Ref. [9] and with the value of the parameter describing the low x -behaviour of the non-singlet neutrino structure function xF_3 , which was obtained from the fit to the CCFR data in Refs. [56,57]. For the obtained values of the

⁵We especially underline this point, since Eq.(4.2) is often used for theoretical estimates.

parameters, which describe the valence u - and d -quarks behaviour at high x , the relation $b_d = a_u + 1$ holds with good precision, in line with the quark counting rules. Meanwhile, the absolute values of these parameters deviate from the quark counting rules predictions $b_u = 3$, $b_d = 4$. This disagreement can also be due to the QCD evolution, moreover for the non-singlet distribution the evolution effect is stronger at high x .

As one can see from Table II, the systematic errors on the parameters describing the valence u -quark distributions at high x and the sea quarks distributions at low x are especially large. At the same time the ratio of the total error to the pure statistical one is $O(1)$ for any fitted parameter, that guarantees their unbiasedness. In order to estimate the sensitivity of the parameters values to the approach used for the account of the systematic errors we performed the fit using the SCE and the fit with the statistical and systematic error combined in quadrature. Results of these fits are also given in Table II. One can see, that in the SCE fit the central values of some parameters are shifted by more, than two standard deviations, as compared with the CME fit and the shift is larger for the parameters with large ratio of the systematic errors to the statistical ones, in particular, for b_u and γ_u^2 . Nevertheless, the SCE fit provides correct estimate of the parameters, the only shortcoming of the SCE is that the SCE errors may be several times larger, than the CME errors. In our analysis maximal ratio of these errors is about 5 and within the errors the results of both fits agree. At the same time the fit with the statistical and systematic errors combined in quadrature does may give incorrect estimate of the parameters, since the data correlation information is lost in this case. As a result, the central values of some parameters, in particular, b_G and a_{sd} , obtained from this fit are shifted from the CME fit results by the statistically significant values (see Table II). Some parameters errors obtained in these two fits are very different also, e.g., the errors on $\alpha_s(M_Z)$ and the parameters describing the gluon distribution at high x . These differences evidently may lead to the fake disagreements with another experimental results and cause discussions on new physics manifestation, if the results of the fit performed without the account of the data correlations are used for the comparison. (The example of resolution of such “disagreement” encountered in the comparison of the SLAC-BCDMS and LEP data on α_s was given in Ref. [26]).

V. THE EXPERIMENTAL PDFS UNCERTAINTIES

The fitted PDFs with their experimental errors, including both statistical and systematic ones are given in Fig. 3, and the relative experimental errors on the PDFs are given in Fig. 4. To estimate the separate contribution of the systematic errors to the total ones we calculated the parameters dispersions keeping the central values of the fitted parameters, but without the account of systematic errors on the data. Then we extracted these reduced dispersions from the total dispersions of the parameters and took the square roots of these differences as the systematic errors on the parameters. The ratio of systematic errors on the selected PDFs to their statistical errors is given in Fig. 5. As it was noted above, the systematic errors impact is more important for the u -quark distribution at all x in question and for d -quark distribution at low x . The PDFs errors, as well as their parameters errors, depend on the approach used for the accounting of systematic errors. The PDFs errors obtained in the CME and SCE fits are compared in Fig. 6 and one can see, that for the latter the errors

are several times larger generally. The errors on PDFs obtained from the CME fit in our earlier analysis of Ref. [9] are also given in the same figure. In that analysis we used data of Refs. [2,3,5,6] with $Q^2 > 9 \text{ GeV}^2$ and $W > 4 \text{ GeV}$. At small and moderate x the errors on PDFs obtained in the earlier analysis are several times larger, than the PDFs errors obtained in the present analysis. At high x these errors are of the same order, and for some PDFs the earlier analysis errors are even smaller. This occurs due to in the analysis of Ref. [9] the HT contribution was fixed at zero, that decreased the PDFs errors. The correlation coefficients matrix for the PDFs parameters is given in Table III and the selected PDFs correlation coefficients are given in Fig. 7. The correlations are larger for the valence and sea quarks distributions. This can be readily understood, since these distributions contribute to the charged leptons DIS structure functions as the sum and hence can be separated hardly. Due to the large correlations between some PDFs the ratio of the systematic errors on their linear combinations to the statistical errors on these combinations may be not proportional to such ratios for the PDFs themselves. For example, as one can see in Fig. 5, the relative systematic errors on the sum of non-strange quarks distributions at low x are significantly smaller, than for the u - and d -quarks distributions separately.

The relative experimental error on the gluon distribution rises with x due to rapid falloff of the distribution itself. The prompt photon data were often used to better confine the gluon distribution at high x , but the prompt photon production data, which appeared recently, turned out to be in disagreement with the earlier data (see review [58]). Besides, it was shown, that in the theoretical analysis of this process large uncertainties occur (see review [59]). For these reasons one cannot use the prompt photon data for pinning down the gluon distribution in a consistent way. In our analysis the gluon distribution at low x is determined by the slope of the structure function F_2 on Q (see Ref. [60]) and at high x , from the partons momentum conservation. The experimental errors on the sea quarks distributions are also rather large, since we did not use in the analysis the Drell-Yan process data.

Unfortunately, the obtained PDFs and their errors suffers from definite model dependence. For example, if one releases the constraint $a_{su} = a_{sd} = a_{ss}$, the quarks distributions errors at low x rise significantly. Analogous effect is observed, if more polynomial factors are added to the starting PDFs. Such model dependence is inevitable, since it is impossible to determine a continuous distribution from limited number of measurements without additional constraints. The model dependence is stronger for the PDFs correlated with another PDFs, e.g., for the sea and valence quarks distributions, while the model dependence is weak for the sum of these distributions. The gluon distribution is also insensitive to the variation of the quark distributions due to rather weak correlation with the latter (see Table III).

The MRST and CTEQ PDFs are given in Fig. 3 in comparison with ours, although the comparison is incomplete, since the errors on the MRST and CTEQ PDFs are unknown. Note, that the difference between the MRST and CTEQ PDFs almost everywhere is smaller, than our PDFs errors. At high x it may occur due to those collaborations use in the analysis more data, but more probable explanation is that the MRST and CTEQ collaborations get similar results due to they use similar data sets. In particular, this means, that the difference between the MRST and CTEQ PDFs cannot be used as the estimate of the PDFs uncertainty. In the whole, with the account of our PDFs errors, there is no striking disagreement of our PDFs with the MRST and CTEQ ones. Our gluon distribution is slightly higher, than the MRST one at low x , but this disagreement is statistically insignificant.

Excess of our sea quarks distributions over the MRST and CTEQ ones at low x is statistically significant, but there are several reasons for it. Firstly, both collaborations use massless scheme for the account of the heavy quarks contribution, that can lead to the overestimation of this contribution, and the corresponding underestimation of the light quarks contribution at low x . Secondly, the MRST and CTEQ collaborations use in the analysis the CCFR neutrino data of Ref. [61], which confine the sea quarks contribution and which were recently corrected by the authors just at low x (see Ref. [62]). Finally, the discrepancy between the MRST and CTEQ PDFs is of the order of discrepancy between those PDFs and ours, i.e. one needs to perform a detailed analysis of all parametrizations to clarify this discrepancy. Excess of the u - and d -quarks distributions over the MRST and CTEQ ones at $x \lesssim 0.3$ is most statistically significant. We checked, that that this excess occurs due the MRST and CTEQ collaborations renormalize the BCDMS data by 1-2% downward. Since we do not apply such renormalization, our parametrization for F_2 , as well as the u - and d -quarks distributions, lays higher. Besides, we applied the TMC correction and the correction on the Fermi-motion in deuterium, that also leads do the rise of the quarks distributions at moderate x . Note, that this excess may help to explain the excess of the TEVATRON jet production cross section data at transverse energies of $E_T = 200 - 400$ GeV over the QCD predictions, since this cross section gets large contribution from the quark-quark scattering at $x \sim 0.2$.

The comparison of our PDFs errors with the errors on PDFs of Ref. [10] is given in Fig. 6. One can see that, despite of that in the analysis of Ref. [10] an additional NMC data on the neutron and proton structure functions ratio and the CCFR neutrino data are used, our PDFs errors are smaller generally. We ascribe this difference to that in the analysis of Ref. [10] the SCE was used in the fit. This conclusion is supported by the comparison of the structure function F_2 band, calculated from the PDFs of Ref. [10], with the data used in that fit. The comparison is given in Fig. 8. One can see that the most left point error is smaller, than the error on the F_2 parametrization of Ref. [10] for this point, i.e. SCE applied for that analysis uses information given by this measurement inefficiently. The qualitative explanation of such behaviour of the SCE is that for this estimator the fitted parameters systematic errors are basically determined by the data points with the largest systematic errors. The CME used in our analysis is more efficient, than SCE and, as one can conclude from Fig. 8, our error on the F_2 parametrization is basically confined by the point with the lowest systematic error. The difference of the SCE and CME PDFs errors is more the more is the relative contribution of the systematic errors to the total one. As a consequence this difference is especially large for the u -quark distribution and it is demonstrative, that the error on the u -quark distribution of Ref. [10] almost coincide with the u -quark distribution errors obtained from our SCE fit (see Fig. 6). The error on d - and u -quarks distributions ratio at high x given by our PDFs is also smaller, as compared with this error given by the PDFs of Ref. [10] (see Fig. 9).

VI. THE THEORETICAL UNCERTAINTIES

The theoretical uncertainties inherent for a phenomenological analysis cannot be ultimately defined, since in the study progress the set of such uncertainties may increase or

decrease. In our analysis we accounted for the following sources of the theoretical uncertainties:

MC – the change of the c -quark mass by 0.25 GeV;

SS – the change of the strange sea suppression factor by 0.1, in line with the estimate given by the NuTeV collaboration [48];

TS – the change of the heavy quarks threshold values from $m_{c,b}$ to $\sqrt{6.5}m_{c,b}$, in accordance with the consideration of Sec.II;

RS – the change of the renormalization scale in evolution the equations from $Q/2$ to $2Q$;

DC – the change of the deuterium nuclear model based on the account of Fermi-motion [50] on the phenomenological model of Ref. [63]. In view of the discussion of Refs. [64,65] on the applicability of the model of Ref. [63] to the light nuclei, one may suppose that this change leads to the overestimation of the corresponding error.

These changes were made in turn and the fitted parameters shifts for each change were taken as the theoretical errors on the parameters. Sometimes in other similar analysis the PDFs theoretical errors due to the α_s and HT uncertainties are estimated using the same approach. In our analysis these errors are included in the total experimental errors, since both α_s and the HT contribution are fitted. We underline, that the scales of the considered theoretical errors are rather conventional, since they are based on the “reasonable” estimates of the model uncertainties. For this reason the theoretical errors should be accounted for with certain cautions.

VII. THE α_s VALUE AND THE HT CONTRIBUTION

We obtained from the fit the value $\alpha_s(M_Z) = 0.1165 \pm 0.0017(\text{stat} + \text{syst})$. The experimental error on α_s obtained in our analysis is two times less, than in the NLO analysis of similar data set described in Ref. [23], where the value $\alpha_s(M_Z) = 0.1160 \pm 0.0034(\text{exp})$ was obtained. The contributions of separate sources of the theoretical errors on our value of $\alpha_s(M_Z)$ are given in Table IV. One can see, that the largest contributions give uncertainties of the QCD renormalization scale and the heavy quarks threshold values (especially for b -quark). Combining all these contributions in quadrature, we obtain

$$\alpha_s(M_Z) = 0.1165 \pm 0.0017(\text{stat} + \text{syst}) \pm_{0.0034}^{0.0026}(\text{theor}), \quad (7.1)$$

which agrees with the modern world average $\alpha_s(M_Z) = 0.1184 \pm 0.0031$ given in Ref. [66]. Our estimate of the α_s value is insensitive to the complication of the PDFs form, since it is almost uncorrelated with the PDFs parameters, in particular, with the gluon distribution ones (see Table III).

As it was recently reported in Ref. [24], the net partons momentum for the PDFs, obtained from the data set similar to one used in our analysis, is not equal to 1, if one does not cut the data with $Q^2 \lesssim 10 \text{ GeV}^2$. In particular, the net partons momentum obtained from the analysis of the world charged leptons DIS data with $Q^2 \geq 3 \text{ GeV}^2$ is

$\langle x \rangle \approx 1.08 \pm 0.02$, as it is given in Ref. [24]. The conclusion drawn from this observation is that the DIS data at low Q are irrelevant for the NLO QCD analysis and reliable results can be obtained from the fit to the data with $Q^2 \geq 10 \text{ GeV}^2$, $W^2 \geq 10 \text{ GeV}^2$ only. The value of $\alpha_s(M_Z) = 0.114 \pm 0.002$ obtained in this analysis differs from ours. In order to perform comparison with this result, we repeated our fit without imposing the momentum conservation constraint on the PDFs and obtained that at $Q^2 = 9 \text{ GeV}^2$ the net partons momentum is $\langle x \rangle = 0.979 \pm 0.029$, which agrees with 1 and differs from the results of Ref. [24]. For this reason we cannot support the conclusion of Ref. [24] about irrelevance of the low Q charged leptons DIS data for the NLO QCD analysis. For more detailed comparison we performed the test fit with the cuts of Ref. [24] and also obtained the lower value $\alpha_s(M_Z) = 0.1098 \pm 0.0055$, but with the error, which is significantly larger, than one obtained in Ref. [24], and the α_s value obtained in this test fit is in agreement with (7.1) within the errors. The observed difference of the α_s errors evidently occurs due to in our analysis we simultaneously fit both the α_s value and the HT contribution to F_2 . As it was shown in Refs. [26,16], the latter are strongly correlated, that certainly leads to the rise of the parameters errors. In support of this conclusion, if in our test fit the HT contribution is fixed, the α_s error falls from 0.0055 to 0.0014. However, the results of the fit with the HT fixed are model dependent and essentially the decrease of the experimental error is accompanied by the uncontrolled rise of the theoretical errors.

The HT contributions to the nucleon structure functions F_L and to the proton and neutron structure functions F_2 are given in Fig. 10 and in Table V. It is interesting that up to minimal x the twist 4 contribution to the structure function F_2 is non-zero, that coincides with the results of Ref. [67] on the analysis of the NMC data. The deviation of the F_L twist 4 contribution off zero at low x is even more significant. As one can see from Table V, the HT contributions to F_2 and to F_L at low x are very sensitive to the approach used to account for the systematic errors on data. This is due to at low x the HT contributions are determined from the comparison of the data at the kinematical edges of different experiments, where the systematic errors are largest as a rule. Note, that the HT parameters errors obtained in the CME fit are 2-3 times smaller, than in the SCE fit, as well as the PDFs parameters errors.

The twist 4 contributions obtained at the different values of the QCD evolution equations renormalization scale μ_R are given in Fig. 10. The evident dependence of H_2 on μ_R at low x indicates that in this x -region the twist 4 contribution to F_2 can simulate the effect of the NNLO corrections to the splitting functions P . Analogous effect for the structure function $x F_3$ was demonstrated in Ref. [68], while the direct observation of the re-tuning of the twist 4 contribution to $x F_3$ due to the account of the NNLO corrections was reported in Ref. [21]. At the same time the μ_R dependence of H_L and of H_2 at high x is not so strong. The explanation of such behaviour is given in Ref. [34]. As it was also shown there, due to the HT contribution can partially absorb the NNLO corrections effects, the μ_R dependence of the α_s value obtained in the simultaneous fit of the HT contribution and α_s is weaker, than in the fit with the HT contribution fixed. In particular, due to this absorption, the α_s renormalization scale error obtained in our analysis is smaller, than in the analysis of Ref. [24].

The difference of the HT contributions to the proton and neutron structure functions F_2 is given in Fig. 11. One can see, that at low x these contributions coincide within errors. This

is in disagreement with the results of Ref. [69]. In that paper the data on the difference of the proton and neutron structure functions F_2 are compared with the calculations based on the standard PDFs and found to be lower than that calculations at $x \sim 0.3$. This discrepancy was attributed to the existence of the large HT contribution to the difference of the proton and neutron structure functions F_2 . We do observe the statistically significant deviation of $H_2^n - H_2^p$ off zero, but at $x \sim 0.7$ instead of $x \sim 0.3$. Unfortunately, this difference strongly depends on the deuterium nuclear corrections model at large x (see Fig. 11) and in order to obtain a reliable estimate of the twist 4 contribution to F_2^n an additional comparative analysis of the deuterium models is needed.

VIII. THE PARTON LUMINOSITIES AT THE FNAL AND LHC COLLIDERS

All errors on the hard processes cross sections due to the PDFs uncertainties are concentrated in the parton luminosities (PLs), defined as

$$L_{ij}(M) = \frac{1}{s} \int_{\tau}^1 \frac{dx}{x} q_i(x, M^2) q_j(\tau/x, M^2),$$

where s is the s.c.m. energy squared; M is the produced mass; $\tau = M^2/s$; i and j mark the parton species. Since the PLs errors strongly depend on the latter, one is to estimate the impact of the PDFs errors on the calculated cross sections errors in each particular case. Our PDFs total errors, comprised of the theoretical errors combined with the experimental ones are given in Fig. 4. Despite of that the data set used for the extraction of our PDFs is limited by the DIS data, the PDFs errors are rather small at low x , i.e. in the region especially important for the FNAL and LHC experiments. The valence quarks distributions errors are small at high x also (see Fig. 4). The experimental errors dominate for the sea and gluon distributions at high x only (note, that this is not the case for the SCE fit, as one can see from the comparison of Fig. 4 and Fig. 6). As one can see from Fig. 12, the dominating source for the gluon distribution at low x is the RS uncertainty, for the sea distribution at low x , the MC one, for the d -quark distribution, the DC one. Remind, that in our analysis the errors due to the uncertainties of the α_s value and the HT contribution are included into the experimental error. To estimate their contribution to the total error we re-calculated the PDFs dispersions fixing the α_s value and the HT contribution by turn, then extracted obtained dispersions from the nominal dispersions calculated with these parameters released. The square roots of these differences were taken as the PDFs errors due to the α_s and the HT uncertainties respectively. The ratios of these errors to the total PDFs errors are also given in Fig. 12. One can see, that the α_s uncertainty affects the gluon distribution only, while the HT uncertainty contributes to the errors of all PDFs.

The errors on the PLs relevant for the most common processes at the energy of the FNAL collider are given in Fig. 13. The upper limit of the pictures was chosen so that the PLs at the upper limit is ~ 0.01 1/pb, i.e. corresponds to the maximal sensitivity of the planned experiments. One can see, that at the FNAL collider energy the theoretical errors dominate over the experimental ones at $M \lesssim 0.2$ TeV and vice versa at $M \gtrsim 0.2$ TeV. The total PLs errors for the FNAL collider generally do not exceed 10% at $M \lesssim 0.2$ TeV, while for the quark-antiquark PL the total error is smaller, than 10% almost for all M in question.

The PLs pictures for the LHC energy, given in Fig. 14, approximately reproduce the FNAL pictures with the produced mass M scaled in 5 times and the quark-antiquark PL replaced by the quark-quark PL.

Due to the PDFs correlations generally are not small (see Fig. 7), the account of these correlations may affect the calculated hard processes cross sections errors. In some cases the PLs errors may cancel in their ratio, as in the example given in Table VI. Calculating the theoretical errors on the hard processes cross sections one is also to take into account the correlations of PDFs with the elementary processes cross sections, if the latter depend on the parameters responsible for the PDFs theoretical uncertainties. Besides, the RS PDFs uncertainty may be compensated by the NNLO corrections to the elementary processes cross sections.

IX. CONCLUSION

Significant part of the studies planned for the next generation hadron-hadron and lepton-hadron colliders is devoted to the precise Standard Model checks (see, e.g., review [70]). Such studies certainly imply careful control of all possible uncertainties, including the PDFs errors. The PDFs obtained in our analysis are supplied by the experimental and theoretical errors and can be used for the correct estimate of the calculated hard processes cross sections uncertainties, necessary for a precise phenomenological comparison aiming to detect a manifestation of new physics (e.g., compositeness in proton-proton and electron-proton collisions, the partons recombination at low x , precise determination of the W and Z masses, etc.). A particular feature of our PDFs is that they were obtained using efficient estimator and, as a result, have minimal errors. The convenient code allowing to account for the PDFs uncertainties in the Monte Carlo calculations is accessible through the computer network⁶. Using the current version of this code one can obtain the random Gaussian smeared PDFs values with the account of the experimental and the theoretical uncertainties and their correlations. The special parameters allow one to scale the dispersions corresponding to the separate sources of the PDFs uncertainties to give user the possibility to study effects of each uncertainty and vary the confidence level of the errors on the calculations results.

Author is indebted to A.L. Kataev and S.A. Kulagin for the careful reading of the manuscript and valuable comments, S. Keller and W.J. Stirling for the interesting discussions. The work was partially supported by the RFBR grant 00-02-17432. The final part of the work was completed during the visit to CERN and author is grateful to the staff of the TH division for providing good working conditions.

⁶The WWW address is <http://www.ihep.su/~alekhin/pdf99>

REFERENCES

- [1] L. W. Whitlow, E. M. Riordan, S. Dasu, S. Rock and A. Bodek, Phys. Lett. **B282**, 475 (1992).
- [2] A. C. Benvenuti *et al.* [BCDMS Collaboration], Phys. Lett. **B223** (1989) 485;
A. C. Benvenuti *et al.* [BCDMS Collaboration], Phys. Lett. **B237** (1990) 592.
- [3] M. Arneodo *et al.* [New Muon Collaboration], Nucl. Phys. **B483** (1997) 3 [hep-ph/9610231].
- [4] M. R. Adams *et al.* [E665 Collaboration], Phys. Rev. **D54** (1996) 3006.
- [5] S. Aid *et al.* [H1 Collaboration], Nucl. Phys. **B470**, 3 (1996) [hep-ex/9603004].
- [6] M. Derrick *et al.* [ZEUS Collaboration], Z. Phys. **C72**, 399 (1996) [hep-ex/9607002].
- [7] A. D. Martin, R. G. Roberts, W. J. Stirling and R. S. Thorne, Eur. Phys. J. **C14**, 133 (2000) [hep-ph/9907231].
- [8] H. L. Lai *et al.* [CTEQ Collaboration], Eur. Phys. J. **C12**, 375 (2000) [hep-ph/9903282].
- [9] S. I. Alekhin, Eur. Phys. J. **C10** (1999) 395 [hep-ph/9611213].
- [10] M. Botje, Eur. Phys. J. **C14**, 285 (2000) [hep-ph/9912439].
- [11] S. I. Alekhin, Preprint IFVE-2000-17 (2000) [hep-ex/0005042].
- [12] B. L. Ioffe, V. A. Khoze and L. N. Lipatov, “Hard Processes. Vol. 1: Phenomenology, Quark Parton Model,” *Amsterdam, Netherlands: North-Holland (1984) 340p.*
- [13] K. G. Wilson, Phys. Rev. **179**, 1499 (1969).
- [14] H. Georgi and H. D. Politzer, Phys. Rev. **D14**, 1829 (1976).
- [15] A. P. Bukhvostov, E. A. Kuraev and L. N. Lipatov, Yad. Fiz. **38**, 439 (1983).
- [16] S. I. Alekhin, Eur. Phys. J. **C12**, 587 (2000) [hep-ph/9902241].
- [17] V. N. Gribov and L. N. Lipatov, Sov. J. Nucl. Phys. **15**, 438 (1972);
V. N. Gribov and L. N. Lipatov, Sov. J. Nucl. Phys. **15**, 675 (1972);
G. Altarelli and G. Parisi, Nucl. Phys. **B126**, 298 (1977);
Y. L. Dokshitzer, Sov. Phys. JETP **46**, 641 (1977).
- [18] J. Sanchez Guillen, J. Miramontes, M. Miramontes, G. Parente and O. A. Sampayo, Nucl. Phys. **B353**, 337 (1991);
W. L. van Neerven and E. B. Zijlstra, Phys. Lett. **B272**, 127 (1991), *ibid.* **B273**, 476 (1991), *ibid.* **B297**, 377 (1992);
W. L. van Neerven and E. B. Zijlstra, Nucl. Phys. **B382**, 11 (1992).
- [19] S. A. Larin, T. van Ritbergen and J. A. Vermaseren, Nucl. Phys. **B427**, 41 (1994);
S. A. Larin, P. Nogueira, T. van Ritbergen and J. A. Vermaseren, Nucl. Phys. **B492**, 338 (1997) [hep-ph/9605317];
A. Retey and J. A. Vermaseren, hep-ph/0007294 (2000).
- [20] W. L. van Neerven and A. Vogt, Nucl. Phys. **B568**, 263 (2000) [hep-ph/9907472];
W. L. van Neerven and A. Vogt, Phys. Lett. **B490**, 111 (2000) [hep-ph/0007362].
- [21] A. L. Kataev, A. V. Kotikov, G. Parente and A. V. Sidorov, Phys. Lett. **B417**, 374 (1998) [hep-ph/9706534].
- [22] A. L. Kataev, G. Parente and A. V. Sidorov, Nucl. Phys. **B573**, 405 (2000) [hep-ph/9905310].
- [23] J. Santiago and F. J. Yndurain, Nucl. Phys. **B563**, 45 (1999) [hep-ph/9904344].
- [24] A. Vogt, Nucl. Phys. Proc. Suppl. **79**, 102 (1999) [hep-ph/9906337].
- [25] W. Furmanski and R. Petronzio, Z. Phys. **C11**, 293 (1982);

- W. Furmanski and R. Petronzio, Phys. Lett. **B97**, 437 (1980);
 G. Curci, W. Furmanski and R. Petronzio, Nucl. Phys. **B175**, 27 (1980).
- [26] S. I. Alekhin, Phys. Rev. **D59**, 114016 (1999) [hep-ph/9809544].
- [27] W. Bernreuther and W. Wetzel, Nucl. Phys. **B197**, 228 (1982), *ibid.***B513**, 758 (1998) (Err);
 S. A. Larin, T. van Ritbergen and J. A. Vermaseren, Nucl. Phys. **B438**, 278 (1995) [hep-ph/9411260];
 K. G. Chetyrkin, B. A. Kniehl and M. Steinhauser, Phys. Rev. Lett. **79**, 2184 (1997) [hep-ph/9706430].
- [28] J. Blumlein and W. L. van Neerven, Phys. Lett. **B450** (1999) 417 [hep-ph/9811351].
- [29] R. M. Barnett *et al.*, Phys. Rev. **D54**, 1 (1996).
- [30] A. D. Martin, W. J. Stirling and R. G. Roberts, Phys. Lett. **B266**, 173 (1991).
- [31] Yndurain, F.J., “Quantum Chromodynamics: an Introduction to the Theory of Quarks and Gluons”, Springer-Verlag, 1983. 227p.
- [32] V. A. Matveev, R. M. Muradian and A. N. Tavkhelidze, Lett. Nuovo Cim. **7**, 719 (1973).
- [33] S. J. Brodsky and G. R. Farrar, Phys. Rev. Lett. **31**, 1153 (1973).
- [34] S. I. Alekhin, Phys. Lett. **B488**, 187 (2000) [hep-ph/9912484].
- [35] J. Blumlein, S. Riemersma, M. Botje, C. Pascaud, F. Zomer, W. L. van Neerven and A. Vogt, in “Hamburg 1995/1996, Future physics at HERA”, p.23 (1996) [hep-ph/9609400].
- [36] “Handbook of Mathematical Functions with Formulas, Graphs, and Mathematical Tables”, ed. by M. Abramowitz and I. A. Stegun., Dover, 1972. 1046p. (Applied Math Series, 55)
- [37] J. C. Collins and W. Tung, Nucl. Phys. **B278**, 934 (1986).
- [38] E. Witten, Nucl. Phys. **B104**, 445 (1976).
- [39] M. A. Shifman, A. I. Vainshtein and V. I. Zakharov, Nucl. Phys. **B136**, 157 (1978).
- [40] M. Gluck, E. Reya and M. Stratmann, Nucl. Phys. **B422**, 37 (1994).
- [41] E. Laenen, S. Riemersma, J. Smith and W. L. van Neerven, Nucl. Phys. **B392**, 229 (1993).
- [42] E. L. Berger and S. J. Brodsky, Phys. Rev. Lett. **42**, 940 (1979);
 J. F. Gunion, P. Nason and R. Blankenbecler, Phys. Rev. **D29**, 2491 (1984).
- [43] L. F. Abbott and R. M. Barnett, Annals Phys. **125**, 276 (1980);
 L. F. Abbott, W. B. Atwood and R. M. Barnett, Phys. Rev. **D22**, 582 (1980).
- [44] A. J. Buras, Rev. Mod. Phys. **52**, 199 (1980).
- [45] V. A. Bednyakov, I. S. Zlatev, Y. P. Ivanov, P. S. Isaev and S. G. Kovalenko, Sov. J. Nucl. Phys. **40**, 494 (1984).
- [46] A. A. Penin and A. A. Pivovarov, Phys. Lett. **B401**, 294 (1997) [hep-ph/9612204].
- [47] B. P. Mahapatra, Preprint SU-PHY-97-03 (1997).
- [48] T. Adams *et al.* [NuTeV Collaboration], Talk given at 34th Recontres de Moriond: QCD and Hadronic Interactions, Les Arcs, France, Mar 1999 [hep-ex/9906037].
- [49] A. D. Martin, W. J. Stirling and R. G. Roberts, Phys. Rev. **D51**, 4756 (1995) [hep-ph/9409410].
- [50] W. B. Atwood and G. B. West, Phys. Rev. **D7** (1973) 773.
- [51] M. Lacombe, B. Loiseau, J. M. Richard, R. Vinh Mau, J. Cote, P. Pires and R. De Tournreil, Phys. Rev. **C21**, 861 (1980);

- M. Lacombe, B. Loiseau, R. Vinh Mau, J. Cote, P. Pires and R. de Turreil, Phys. Lett. **B101**, 139 (1981).
- [52] S. N. Sokolov, Preprint IFVE-88-110 (1988).
- [53] L. W. Whitlow, Report SLAC-0357 (1990).
- [54] W. T. Giele and S. Keller, Phys. Rev. **D58**, 094023 (1998) [hep-ph/9803393].
- [55] D. J. Gross, Phys. Rev. Lett. **32**, 1071 (1974).
- [56] W. G. Seligman, Report NEVIS-292 (1997).
- [57] A. L. Kataev, G. Parente and A. V. Sidorov, Nucl. Phys. **A666**, 184 (2000) [hep-ph/9907310].
- [58] M. Werlen, Preprint LAPTH-734-99 [hep-ph/9906483].
- [59] E. Laenen, G. Sterman and W. Vogelsang, Contributed to 8th International Workshop on Deep Inelastic Scattering and QCD (DIS 2000), Liverpool, England, Apr 2000 [hep-ph/0006352].
- [60] K. Prytz, Phys. Lett. **B311**, 286 (1993).
- [61] W. G. Seligman *et al.*, Phys. Rev. Lett. **79**, 1213 (1997).
- [62] U. K. Yang *et al.* [CCFR/NuTeV Collaboration], hep-ex/0009041 (2000).
- [63] J. Gomez *et al.*, Phys. Rev. **D49** (1994) 4348.
- [64] W. Melnitchouk, I. R. Afnan, F. Bissey and A. W. Thomas, Phys. Rev. Lett. **84**, 5455 (2000) [hep-ex/9912001].
- [65] U. K. Yang and A. Bodek, Phys. Rev. Lett. **84**, 5456 (2000) [hep-ph/9912543].
- [66] S. Bethke, J. Phys. G **G26**, R27 (2000) [hep-ex/0004021].
- [67] M. Arneodo *et al.* [New Muon Collaboration], Phys. Lett. **B309**, 222 (1993).
- [68] S. I. Alekhin and A. L. Kataev, Nucl. Phys. **A666-667**, 179 (2000) [hep-ph/9908349].
- [69] A. Szczurek and V. Uleshchenko, Phys. Lett. **B475**, 120 (2000) [hep-ph/9911467];
A. Szczurek, Talk given at 8th International Workshop on Deep Inelastic Scattering and QCD (DIS 2000), Liverpool, England, Apr 2000 [hep-ph/0006320].
- [70] A. Ahmadov, *et al.*, Proceedings of the Workshop on Standard Model Physics (and more) at the LHC, ed. G. Altarelli and M.L. Mangano, CERN-2000-04 (2000);//
S. Catani *et al.*, hep-ph/0005025.

FIGURES

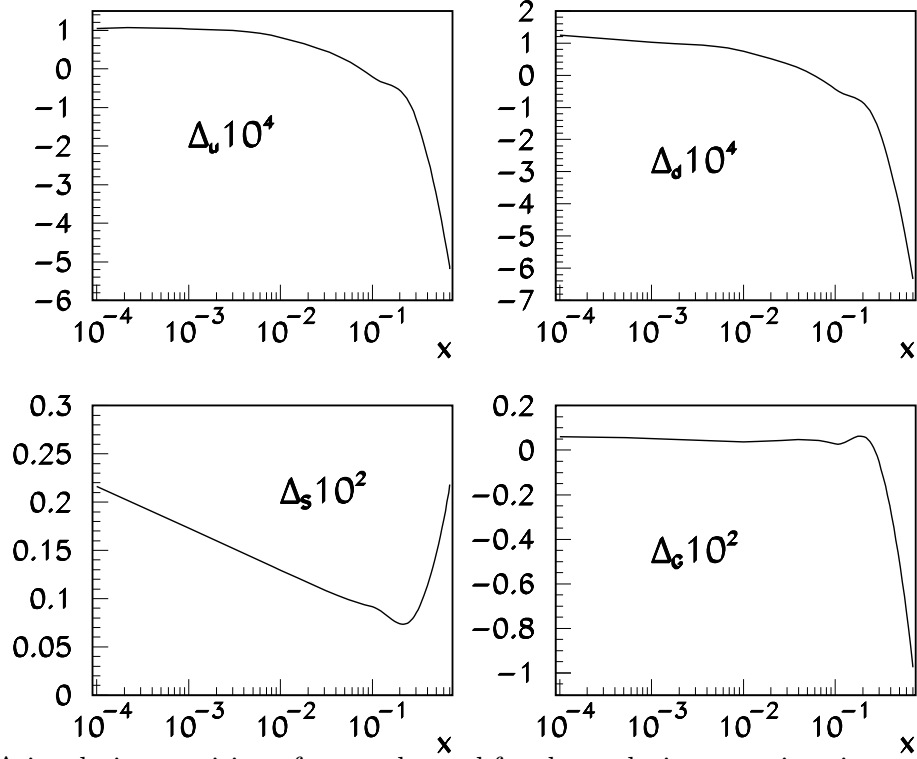


FIG. 1. Δ is relative precision of our code used for the evolution equations integration. Indices u and d correspond to the valence quarks; S , to the sea quarks; G , to gluon.

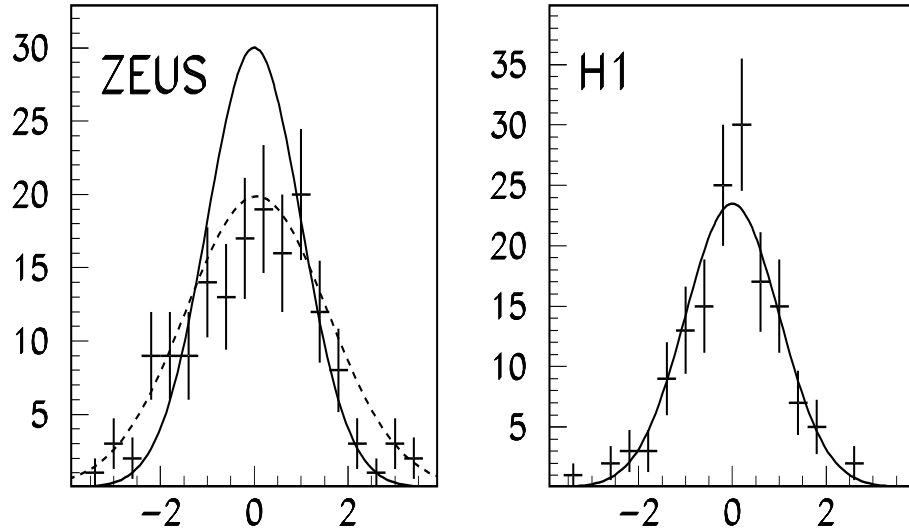


FIG. 2. The distribution of diagonalized residuals for the ZEUS and H1 data (full curves: normal distribution, dashes: the Gauss distribution with the dispersion and the mean equal to the dispersion and the mean of the residuals distribution). All curves are normalized to the number of points in each experiment.

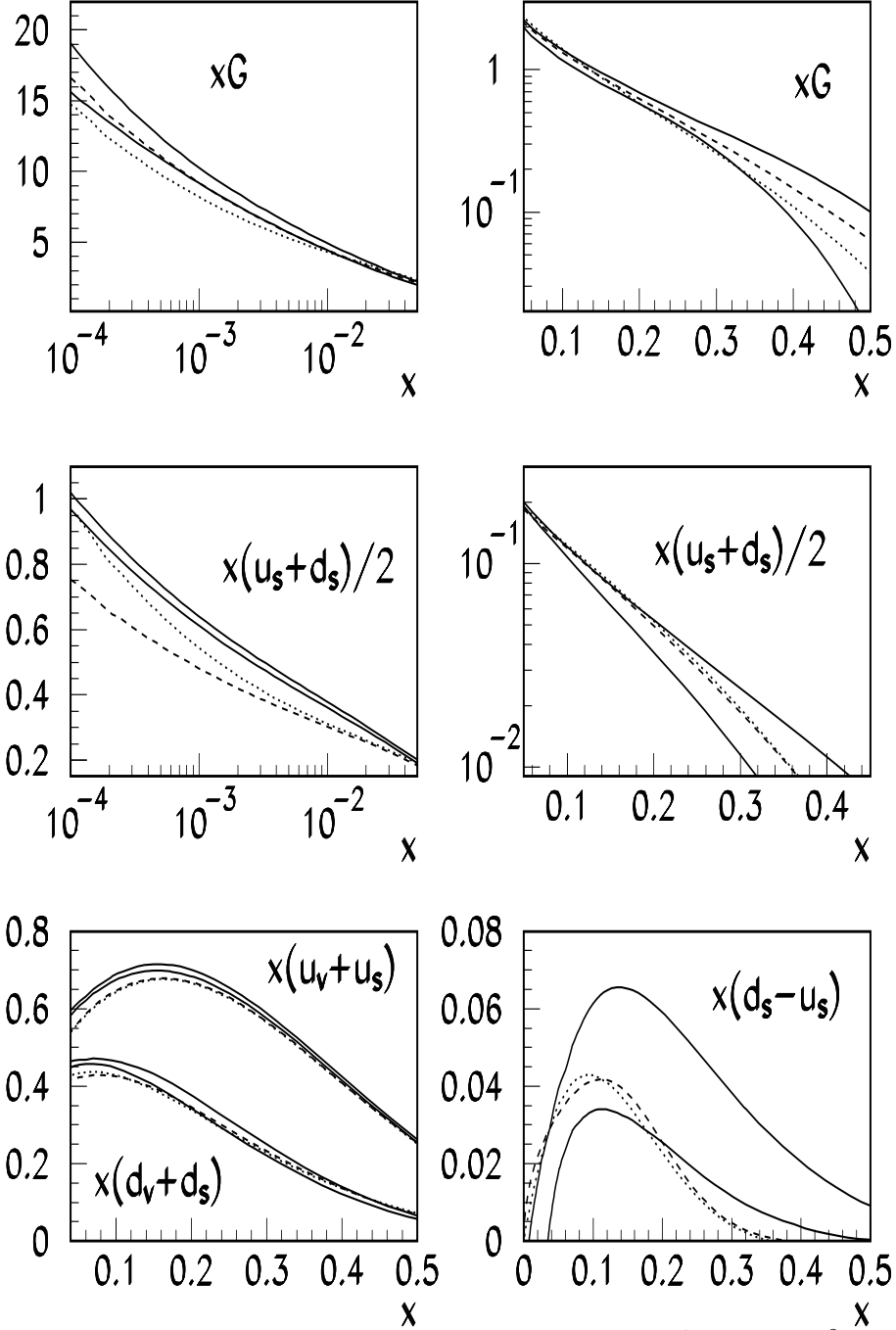


FIG. 3. The 1σ experimental error bands for our PDFs at $Q^2 = 9 \text{ GeV}^2$ (full lines). For comparison the nominal MRST99 (dots) and CTEQ5 (dashes) PDFs are also given.

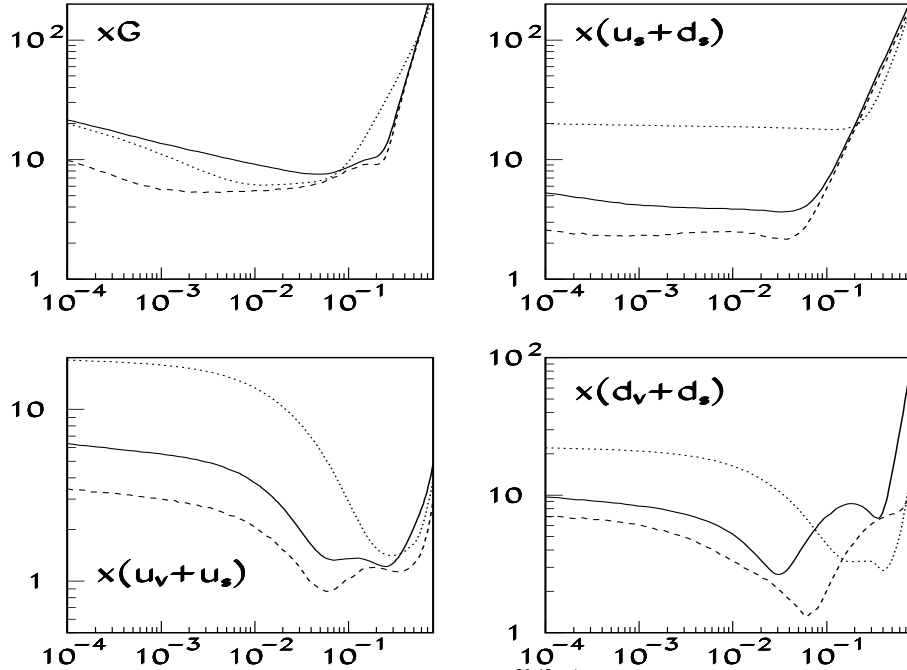


FIG. 4. The relative experimental PDFs errors [%] (full lines: the total errors, dashes: the experimental ones). For comparison the relative experimental errors on the PDFs of Ref. [9] are also given (dots).

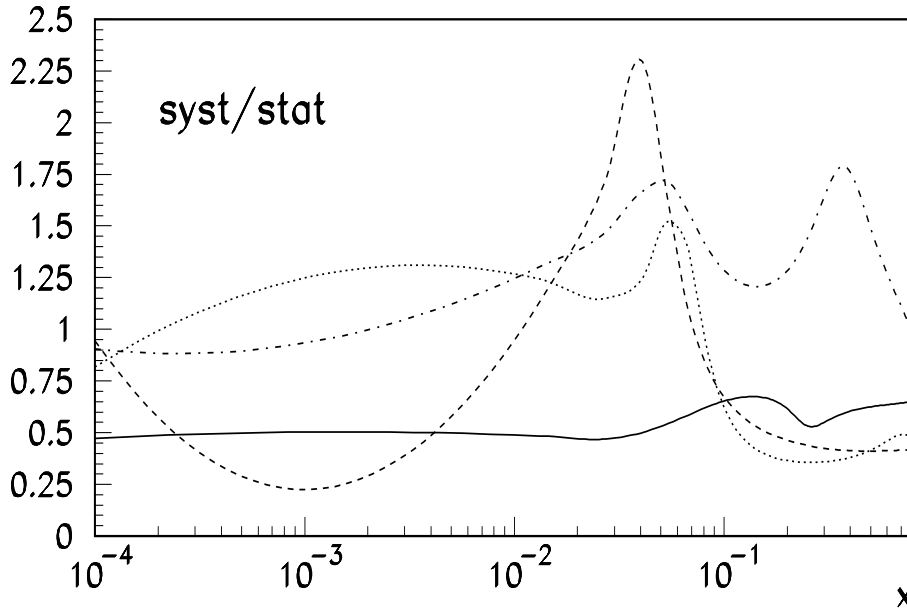


FIG. 5. The ratio of the systematic errors on the fitted PDFs to the statistical ones (full lines: the gluon distribution; dashes: the total sea one; dots: the d -quark one; dotted-dashes: the u -quark one).

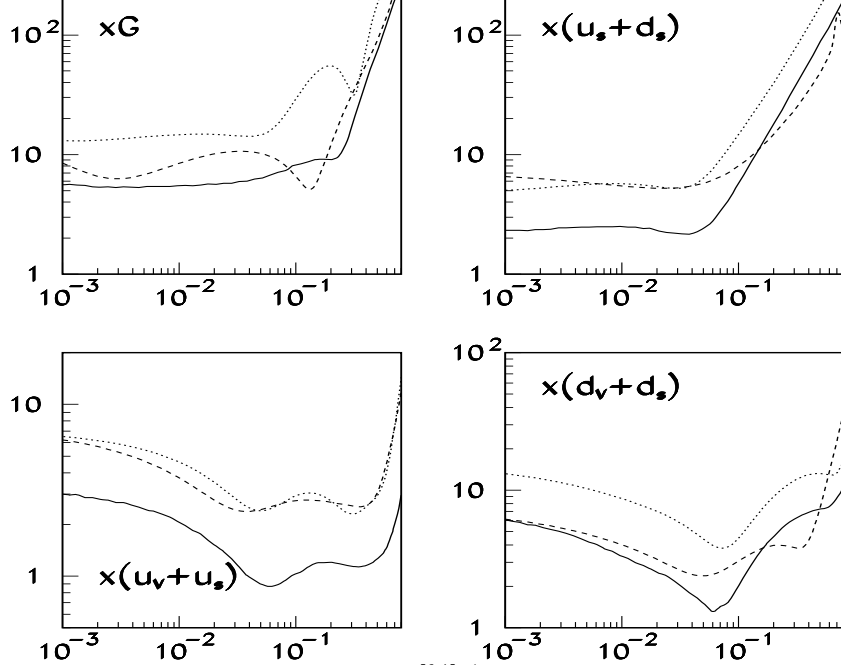


FIG. 6. The relative experimental PDFs errors [%] (full lines: our analysis, dashes: the analysis of Ref. [10]). For comparison the relative experimental PDF errors obtained in our analysis from the SCE fit are also given (dots).

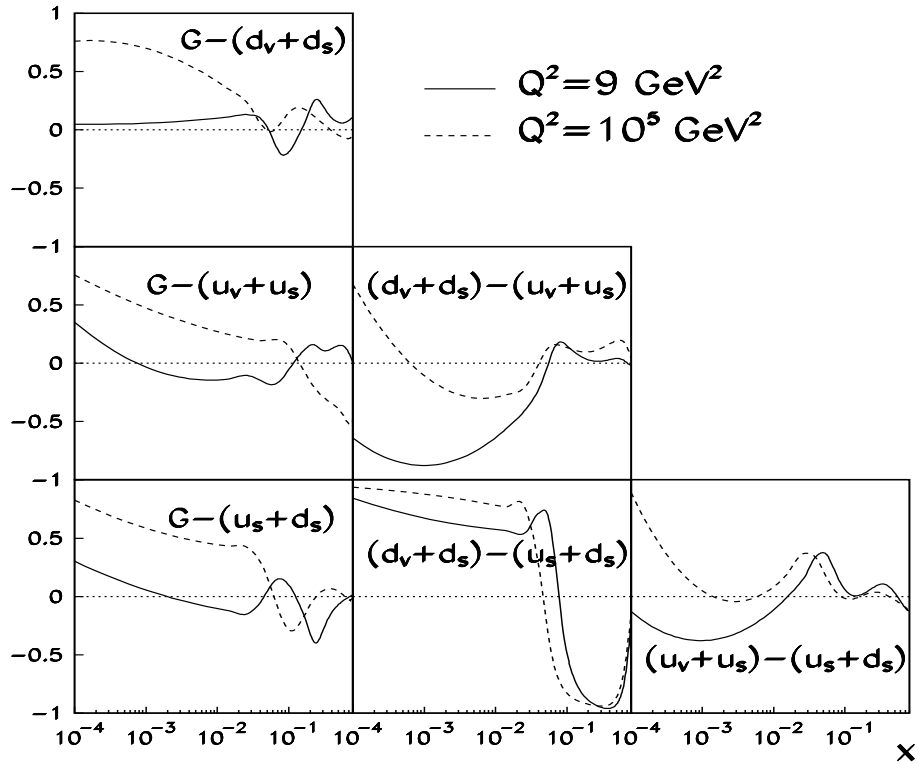


FIG. 7. The PDFs correlation coefficients at different Q^2 .

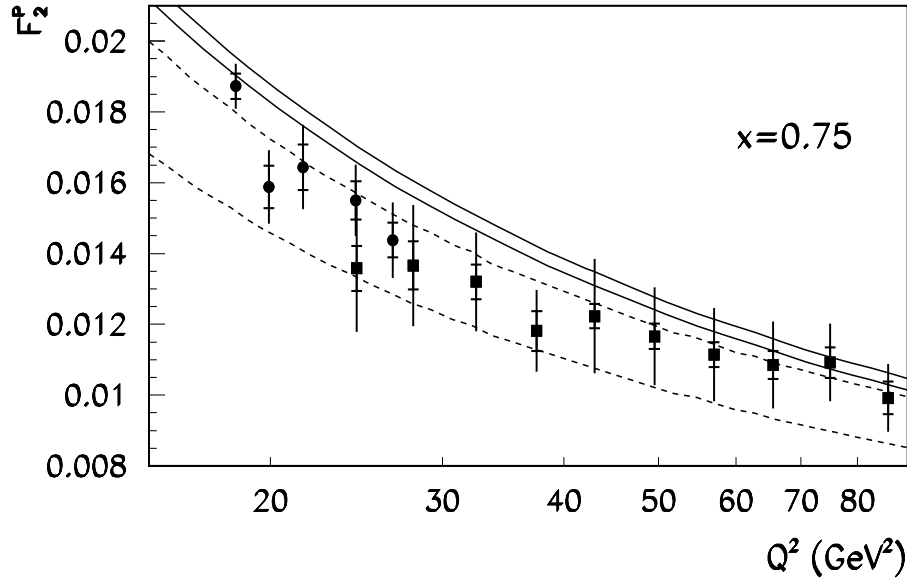


FIG. 8. The 1σ experimental error bands for F_2^p calculated using different PDFs (full line: our PDFs; dashes: the PDFs of Ref. [10]). Circles: the SLAC data; squares: the BCDMS ones.

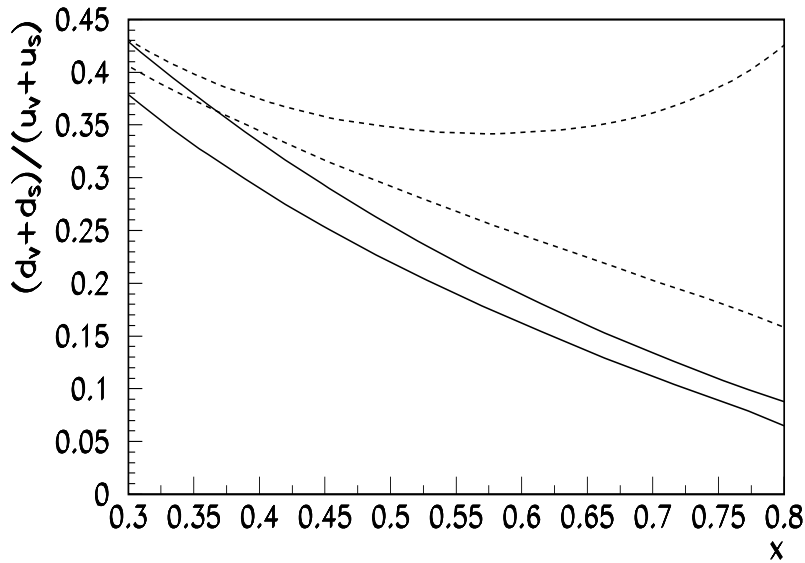


FIG. 9. The 1σ experimental error bands for the ratio of d - and u -quarks distributions at $Q^2 = 9 \text{ GeV}^2$ (full lines: our PDFs; dashes: the PDFs of Ref. [10]).

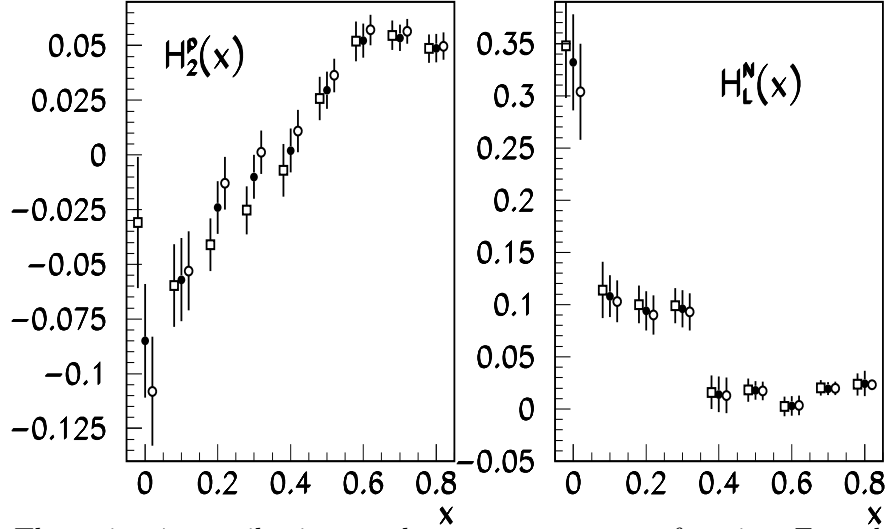


FIG. 10. The twist 4 contribution to the proton structure function F_2 and to the nucleon structure function F_L (full circles: $\mu_R = Q$; open circles: $\mu_R = 2Q$; squares: $\mu_R = Q/2$). For better view the points corresponding to different μ_R are shifted to left-right along the x -axis.

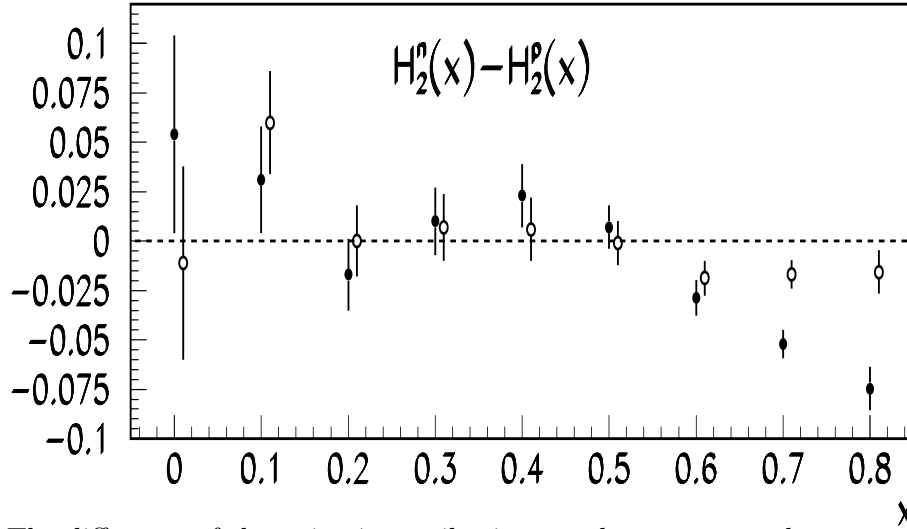


FIG. 11. The difference of the twist 4 contributions to the neutron and proton structure functions F_2 obtained in the fits using the different deuterium models (full circles: the Fermi-motion model; open circles: the model of Ref. [63]). For better view the points corresponding to different models are shifted to left-right along the x -axis.

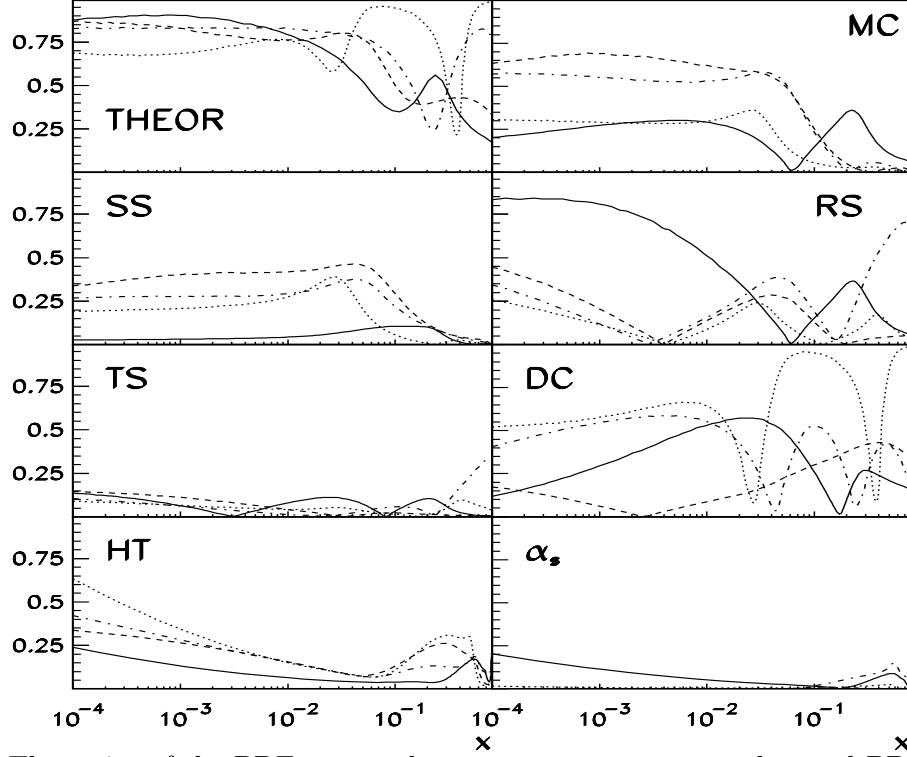


FIG. 12. The ratios of the PDFs errors due to separate sources to the total PDFs errors (full lines: the gluon distribution; dashes: the non-strange sea one; dots: the d -quark one; dotted-dashes: the u -quark one). THEOR means the sum of the MC,SS,RS,TS, and DC contributions.

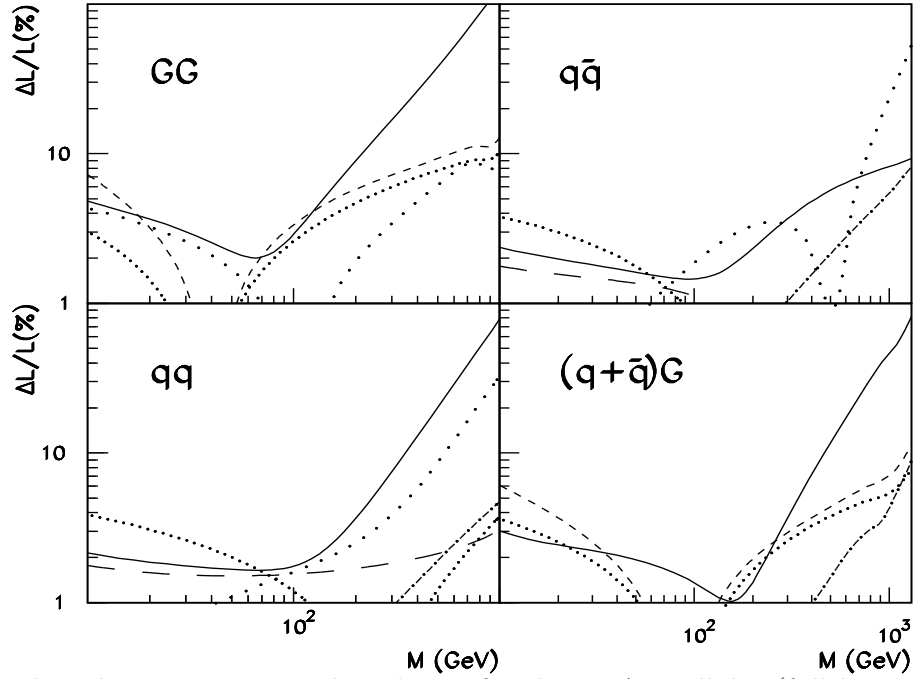


FIG. 13. The relative errors on selected PLs for the FNAL collider (full lines: experimental errors, short dashes: RS; dotted-dashes: TS; sparse dots: DC; dense dots: MC; long dashes: SS). Other notations: $L_{qq} = L_{uu} + L_{dd} + L_{du}$; $L_{q\bar{q}} = L_{u\bar{d}} + L_{d\bar{u}}$; $L_{(q+\bar{q})G} = L_{uG} + L_{\bar{u}G} + L_{dG} + L_{\bar{d}G}$.

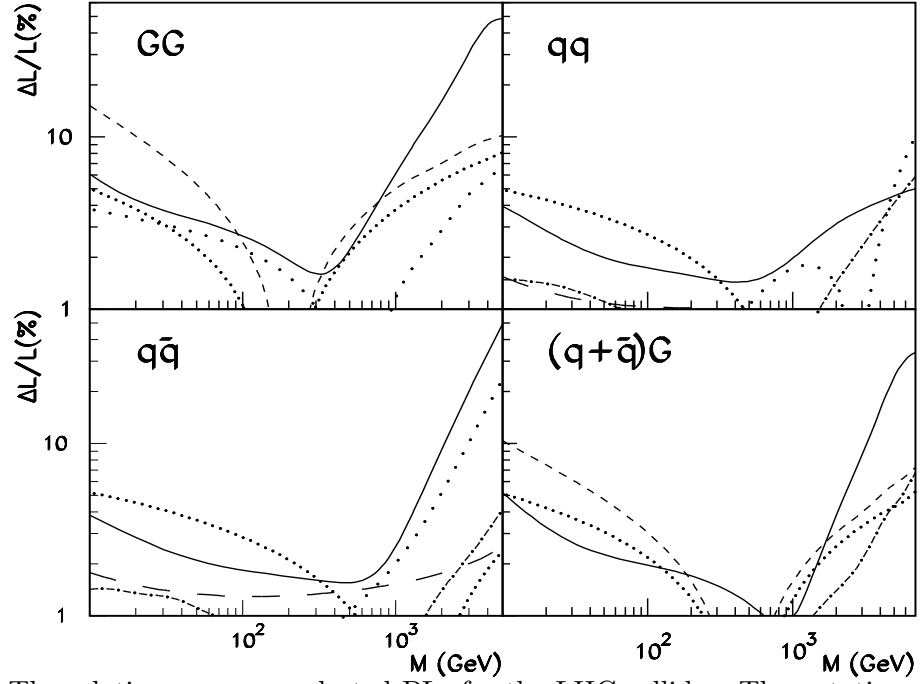


FIG. 14. The relative errors on selected PLs for the LHC collider. The notations are the same as in Fig. 13.

TABLES

TABLE I. Total number of points (NDP), number of independent sources of systematic errors (NSE), χ^2/NDP and the net residual R for each experiment (standard deviation of R is given in parenthesis). Also the renormalization factors ξ for the old SLAC experiments are given.

experiment	NDP/(1 - ξ)[%]		NSE	χ^2/NDP	R
	proton	deuterium			
SLAC-E-49A	58 / 1.8 ± 1.3	58 / -0.4 ± 1.2	3	0.52	-0.05(0.23)
SLAC-E-49B	144 / 2.0 ± 1.3	135 / -0.1 ± 1.3	3	1.20	0.22(0.29)
SLAC-E-87	90 / 2.0 ± 1.2	90 / 0.2 ± 1.2	3	0.91	0.01(0.37)
SLAC-E-89A	66 / 4.2 ± 1.8	59 / 1.2 ± 1.9	3	1.34	-0.18(0.45)
SLAC-E-89B	79 / 1.5 ± 1.2	62 / -0.7 ± 1.2	3	0.82	0.46(0.49)
SLAC-E-139	-	16 / 1.0 ± 1.2	3	0.64	-0.10(0.43)
SLAC-E-140	-	26	4	0.89	0.51(0.86)
BCDMS	351	254	9	1.15	0.07(0.68)
NMC	245	245	13	1.32	0.05(0.62)
H1(94)	-	147	5	0.96	0.11(0.25)
ZEUS(94)	-	188	20	2.14	0.32(0.34)
FNAL-E-665	47	47	10	1.23	0.38(0.38)
Total	1080	1327	79	1.20	0.12(0.22)

TABLE II. The fitted α_s and the PDFs parameters values (I: the CME fit; II: the SCE fit; III: the fit with the statistical and systematic errors combined in quadrature). Given errors on the parameters include both statistical and systematic errors, pure statistical errors are given in parenthesis.

	I	II	III
Valence quarks:			
a_u	$0.693 \pm 0.033(0.027)$	$0.715 \pm 0.114(0.029)$	0.703 ± 0.035
b_u	$3.945 \pm 0.050(0.039)$	$4.119 \pm 0.257(0.038)$	4.037 ± 0.049
γ_2^u	$1.29 \pm 0.44(0.37)$	$1.39 \pm 1.86(0.40)$	1.42 ± 0.49
a_d	$0.725 \pm 0.086(0.082)$	$0.703 \pm 0.172(0.094)$	0.717 ± 0.13
b_d	$4.93 \pm 0.13(0.12)$	$4.83 \pm 0.27(0.17)$	5.00 ± 0.17
Gluon:			
a_G	$-0.225 \pm 0.035(0.031)$	$-0.169 \pm 0.065(0.029)$	-0.135 ± 0.044
b_G	$6.1 \pm 2.1(1.8)$	$4.9 \pm 5.6(1.7)$	4.07 ± 1.3
γ_1^G	$-2.63 \pm 0.83(0.71)$	$-3.41 \pm 0.99(0.45)$	-4.06 ± 0.48
γ_2^G	$4.7 \pm 2.9(2.4)$	$4.44 \pm 3.4(1.3)$	5.41 ± 1.2
Sea quarks:			
A_S	$0.166 \pm 0.011(0.0095)$	$0.167 \pm 0.025(0.011)$	0.167 ± 0.017
a_{sd}	$-0.1987 \pm 0.0067(0.0050)$	$-0.1853 \pm 0.0181(0.0050)$	-0.1833 ± 0.0075
b_{sd}	$5.1 \pm 1.4(1.3)$	$5.4 \pm 2.8(1.4)$	4.9 ± 2.1
η_u	$1.13 \pm 0.11(0.087)$	$1.10 \pm 0.23(0.086)$	1.16 ± 0.16
b_{su}	$10.29 \pm 0.97(0.81)$	$10.56 \pm 3.2(0.83)$	11.2 ± 1.1
$\alpha_s(M_Z)$	$0.1165 \pm 0.0017(0.0014)$	$0.1138 \pm 0.0044(0.0021)$	0.1190 ± 0.0036

TABLE III. The correlation coefficients for the starting PDFs parameters. The largest coefficients are printed in bold.

	a_u	b_u	γ_2^u	a_d	b_d	A_S	a_{sd}	b_{sd}	η_u	b_{su}	a_G	b_G	γ_1^G	γ_2^G	$\alpha_s(M_Z)$	
a_u	1.00															
b_u	-0.84	1.00														
γ_2^u	-0.97	0.92	1.00													
a_d	-0.09	-0.09	0.05	1.00												
b_d	-0.21	0.02	0.19	0.71	1.00											
A_S	-0.14	0.34	0.24	-0.86	-0.54	1.00										
a_{sd}	0.58	-0.45	-0.55	0.37	0.16	-0.46	1.00									
b_{sd}	-0.05	-0.10	0.00	0.97	0.54	-0.88	0.40	1.00								
η_u	0.25	-0.13	-0.23	-0.69	-0.24	0.47	0.01	-0.78	1.00							
b_{su}	0.83	-0.74	-0.86	-0.14	-0.16	-0.24	0.62	-0.10	0.44	1.00						
a_G	0.23	-0.22	-0.23	0.37	0.20	-0.38	0.53	0.37	-0.21	0.18	1.00					
b_G	0.18	-0.17	-0.20	0.11	0.17	-0.08	-0.10	0.06	-0.11	-0.02	0.27	1.00				
γ_1^G	-0.36	0.34	0.36	-0.45	-0.30	0.48	-0.52	-0.44	0.18	-0.30	-0.82	-0.47	1.00			
γ_2^G	0.34	-0.34	-0.36	0.28	0.26	-0.32	0.15	0.23	-0.11	0.20	0.46	0.89	-0.77	1.00		
$\alpha_s(M_Z)$	0.22	-0.31	-0.18	0.01	-0.05	-0.05	0.04	-0.01	0.04	0.17	0.01	-0.39	0.03	-0.18	1.00	

TABLE IV. The $\alpha_s(M_Z)$ theoretical errors due to different sources.

Source	Value
MC	± 0.0003
SS	± 0.0001
RS	$\pm_{0.0024}^{0.0026}$
TS	-0.0020
DC	-0.0012

TABLE V. The fitted twist 4 contributions (I: the CME fit; II: the SCE fit; III: the fit with the statistical and systematic errors combined in quadrature). Given errors on the parameters include both statistical and systematic errors, pure statistical errors are given in parenthesis.

x	I	II	III
$H_2^{\text{P}}:$			
0.	$-0.085 \pm 0.026(0.020)$	$-0.124 \pm 0.051(0.020)$	-0.132 ± 0.035
0.1	$-0.057 \pm 0.019(0.014)$	$-0.107 \pm 0.076(0.014)$	-0.094 ± 0.021
0.2	$-0.024 \pm 0.012(0.0097)$	$-0.057 \pm 0.049(0.010)$	-0.054 ± 0.016
0.3	$-0.010 \pm 0.010(0.0089)$	$-0.027 \pm 0.024(0.0090)$	-0.017 ± 0.015
0.4	$0.002 \pm 0.010(0.0089)$	$0.002 \pm 0.024(0.0090)$	-0.002 ± 0.016
0.5	$0.0292 \pm 0.0085(0.0074)$	$0.041 \pm 0.020(0.0079)$	0.025 ± 0.015
0.6	$0.0522 \pm 0.0078(0.0069)$	$0.068 \pm 0.017(0.0074)$	0.051 ± 0.013
0.7	$0.0535 \pm 0.0061(0.0055)$	$0.074 \pm 0.013(0.0058)$	0.056 ± 0.010
0.8	$0.0488 \pm 0.0064(0.0061)$	$0.0545 \pm 0.0085(0.0060)$	0.0471 ± 0.0085
$H_L^{\text{N}}:$			
0.	$0.332 \pm 0.046(0.033)$	$0.13 \pm 0.11(0.033)$	0.028 ± 0.061
0.1	$0.108 \pm 0.020(0.016)$	$0.117 \pm 0.065(0.016)$	0.118 ± 0.022
0.2	$0.094 \pm 0.019(0.015)$	$0.145 \pm 0.047(0.015)$	0.097 ± 0.021
0.3	$0.096 \pm 0.018(0.016)$	$0.133 \pm 0.031(0.016)$	0.115 ± 0.021
0.4	$0.014 \pm 0.017(0.015)$	$0.040 \pm 0.027(0.015)$	0.033 ± 0.019
0.5	$0.0179 \pm 0.0088(0.0068)$	$0.023 \pm 0.014(0.0069)$	0.015 ± 0.011
0.6	$0.0031 \pm 0.0094(0.0076)$	$-0.016 \pm 0.024(0.0076)$	-0.0033 ± 0.0089
0.7	$0.0195 \pm 0.0064(0.0056)$	$0.008 \pm 0.016(0.0055)$	0.0134 ± 0.0067
0.8	$0.024 \pm 0.012(0.012)$	$0.01 \pm 0.023(0.012)$	0.012 ± 0.014
$H_2^{\text{N}} - H_2^{\text{P}}:$			
0.	$0.054 \pm 0.050(0.041)$	$0.045 \pm 0.112(0.041)$	0.095 ± 0.077
0.1	$0.031 \pm 0.027(0.026)$	$0.041 \pm 0.047(0.026)$	0.003 ± 0.037
0.2	$-0.017 \pm 0.018(0.017)$	$0.024 \pm 0.046(0.017)$	-0.014 ± 0.024
0.3	$0.010 \pm 0.017(0.016)$	$0.052 \pm 0.038(0.016)$	0.014 ± 0.021
0.4	$0.023 \pm 0.016(0.015)$	$0.047 \pm 0.037(0.015)$	0.036 ± 0.019
0.5	$0.0068 \pm 0.011(0.010)$	$0.009 \pm 0.026(0.011)$	0.019 ± 0.016
0.6	$-0.029 \pm 0.0091(0.0086)$	$-0.037 \pm 0.016(0.0092)$	-0.022 ± 0.015
0.7	$-0.052 \pm 0.0073(0.0068)$	$-0.073 \pm 0.014(0.0071)$	-0.055 ± 0.011
0.8	$-0.075 \pm 0.011(0.010)$	$-0.079 \pm 0.014(0.010)$	-0.073 ± 0.013

TABLE VI. The relative errors on the PLs involved in the calculations of the W and Z production cross sections at the FNAL collider ($L_W = L_{u\bar{d}} + L_{d\bar{u}}$, $L_Z = L_{u\bar{u}} + L_{d\bar{d}}$, $L_{W/Z} = (L_{u\bar{d}} + L_{d\bar{u}})/(L_{u\bar{u}} + L_{d\bar{d}})$).

	stat+syst	RS	TS	SS	MC	DC
$\Delta L_W(\%)$	1.5	–	–	1.2	1.1	1.5
$\Delta L_Z(\%)$	1.2	–	–	1.2	1.1	1.5
$\Delta L_{W/Z}(\%)$	0.7	–	–	–	–	–